

# Functioning of intertidal flats inferred from temporal and spatial dynamics of O<sub>2</sub>, H<sub>2</sub>S and pH in their surface sediment

Stefan Jansen · Eva Walpersdorf · Ursula Werner ·  
Markus Billerbeck · Michael E Böttcher · Dirk de Beer

Received: 15 August 2008 / Accepted: 12 January 2009 / Published online: 30 January 2009  
© The Author(s) 2009. This article is published with open access at Springerlink.com

**Abstract** In this article, we describe the dynamics of pH, O<sub>2</sub> and H<sub>2</sub>S in the top 5–10 cm of an intertidal flat consisting of permeable sand. These dynamics were measured at the low water line and higher up the flat and during several seasons. Together with pore water nutrient data, the dynamics confirm that two types of transport act as driving forces for the cycling of elements (Billerbeck et al. 2006b): Fast surface dynamics of pore water chemistry occur only during inundation. Thus, they must be driven by hydraulics (tidal and wave action) and are highly dependent on weather conditions. This was demonstrated clearly by quick variation in oxygen penetration depth: Seeps are active at low tide only, indicating that the pore water flow in them is driven by a pressure head developing at low tide. The seeps are fed by slow transport of pore water over long distances in the deeper sediment. In the seeps, high concentrations of degradation

products such as nutrients and sulphide were found, showing them to be the outlets of deep-seated degradation processes. The degradation products appear toxic for bioturbating/bioirrigating organisms, as a consequence of which, these were absent in the wider seep areas. These two mechanisms driving advection determine oxygen dynamics in these flats, whereas bioirrigation plays a minor role. The deep circulation causes a characteristic distribution of strongly reduced pore water near the low water line and rather more oxidised sediments in the centre of the flats. The two combined transport phenomena determine the fluxes of solutes and gases from the sediment to the surface water and in this way create specific niches for various types of microorganisms.

**Keywords** Intertidal flats · Surface sediment · Permeable sand · Oxygen · Sulphide · Photosynthesis

---

Responsible Editor: Burghard W. Flemming.

---

S. Jansen (✉) · E. Walpersdorf · U. Werner · M. Billerbeck ·  
M. E. Böttcher · D. de Beer  
Max Planck Institute for Marine Microbiology,  
Celsiusstr. 1,  
2835 Bremen, Germany  
e-mail: stefan.jansen@tmo.nl

*Present address:*  
S. Jansen  
P.O. Box 85467, 3508 AL Utrecht, The Netherlands  
e-mail: stefan.jansen@deltares.nl

*Present address:*  
E. Walpersdorf  
Department of Geography & Geology,  
University of Copenhagen,  
Øster Voldgade 10,  
DK-1350 Copenhagen K, Denmark

*Present address:*  
U. Werner  
Advanced Water Management Centre,  
The University of Queensland, St. Lucia,  
Gerhmann Building (60),  
QLD 4072 Queensland, Australia

*Present address:*  
M. Billerbeck  
BMT WBM Pty Ltd,  
490 Upper Edward Street,  
Brisbane 4000 Queensland, Australia

*Present address:*  
M. E. Böttcher  
Leibniz Institute for Baltic Sea Research, Marine Geochemistry,  
Seestr.15,  
18119 Warnemünde, Germany

## 1 Introduction

Intertidal sediments are important sites of organic matter cycling because large surface areas are combined with high microbial activity, both with respect to biomass production and degradation. It is increasingly recognised that sandy sediments can have a high degradation activity in spite of their low organic matter content and bacterial numbers (e.g. De Beer et al. 2005; D'Andrea et al. 2002). They have a higher permeability than more fine-grained sediments, which facilitates advective pore water transport and thereby promotes a high transport of electron donors and acceptors into and out of the sediments. This can lead to areal reaction rates comparable to essentially diffusion-controlled muddy sediments (e.g. Huettel et al. 1998; Böttcher et al. 2000; Rasheed et al. 2003; Werner et al. 2006).

There are several driving forces for advective pore water transport in these sediments. The currents and waves cause hydrostatic pressures which drive pore water movements through the sediments (Precht et al. 2004). Particularly important is the Bernoulli effect created by currents over ripples which causes water inflow in the ripples troughs and outflow at the crests of the ripples (Huettel et al. 1998; Thibodeaux and Boyle 1987). As the inflow into the sediments must be compensated by an outflow elsewhere, a mosaic of surficial circulation cells develops which influence the pore water chemistry in the top 3–10 cm. Secondly, bioturbation and bioirrigation can also cause efficient mixing of the top layers (e.g. Meysman et al. 2005, 2006; Aller 2001; Wethey et al. 2008). Faunal and pressure-driven transport normally takes place over small spatial and temporal scales in the order of centimetres and minutes. For example, due to this effect, the pore water oxygen concentrations in the top 10 cm can increase from 0 to air-saturated values within minutes (De Beer et al. 2005; Werner et al. 2006). The maximum depth at which 'surficial' advective pore water transport takes place varies considerably. Thus, although most of it takes place in the top 10 cm, bioirrigation can also take place at depths up to 30–40 cm.

Besides these small-scale transport mechanisms (skin circulation), the existence of transport processes at much larger temporal and spatial scales was demonstrated for intertidal flats (body circulation; Billerbeck et al. 2006b). This type of transport is driven by a pressure gradient between the pore water level and the low water level during exposure of the flat. The body circulation is characterised by long flow paths (tens of metres) and long residence times (decades) of the pore water (Billerbeck et al. 2006b; Røy et al. 2008). This transport phenomenon drives a pore water flow from the centre of the flat towards the low water line at depths of several metres below the sediment surface.

The two types of transport differ in scale: As stated before, surficial dynamics can range in depth from centimetres to decimetres, whereas horizontal transfers extend for decimetres, and body circulation probably occurs up to 5-m depth over distances exceeding 100 m (Røy et al. 2008). However, the key difference lies in the mechanisms driving the two transport processes.

A wide range of microbial processes occur in intertidal sediments, from primary production to the whole sequence of organic matter mineralisation with various electron acceptors (oxygen, sulphate, nitrate, iron, etc.) and methanogenesis. Most probably, the primary production, aerobic mineralisation and sulphate reduction are the processes dominating the carbon cycle (Billerbeck et al. 2006a, 2007; Werner et al. 2006), whereas methanogenesis and denitrification maybe important for release of greenhouse gasses (CH<sub>4</sub>, N<sub>2</sub>O), but not for element cycling (Røy et al. 2008). Between the islands of Ameland and Spiekeroog, approximately 20 km of potentially seeping low water lines can be mapped out, which could release 130–1,300 mol methane per day. This corresponds to an annual methane release of approximately 0.05–0.5 mmol m<sup>-2</sup>, a very low value compared to, for example, an estimated yearly primary production of 25 mmol C m<sup>-2</sup> and a mineralisation rate of 33 mmol C m<sup>-2</sup> in the North Frisian Wadden Sea (Asmus et al. 1998; Van Beusekom et al. 1999). This rough calculation suggests that methane seepage is of limited importance for the carbon cycle in intertidal flats. However, it is probably very significant for the coastal methane budget. The flux of methane from estuarine waters to the atmosphere of 0.13 mmol m<sup>-2</sup> day<sup>-1</sup> (Middelburg et al. 2002) can be explained by seepage from flats in areas with 1 m of seeping waterline per 50–500 m<sup>2</sup> of water surface.

The distribution of the degradation processes is determined by the availability of electron acceptors and donors, whereas photosynthesis is controlled by light and nutrients. Consequently, the main biogeochemical processes are controlled by transport processes. Skin circulation enhances organic matter mineralisation by efficient filtration of fresh organic matter and various electron acceptors into the permeable sediment. Body circulation can cause seepage of highly concentrated reduced compounds that are normally found in deeper sediment layers (Røy et al. 2008), and this can drive the release of considerable amounts of methane (Middelburg et al. 2002), as was shown to occur at many sites throughout the German and Dutch Wadden Sea (Røy et al. 2008). Of course, the efficient mineralisation of organic matter and transport of degradation products will facilitate benthic photosynthesis by a fresh supply of nutrients.

The transport and biogeochemical processes strongly influence both the biological conversions occurring at the surface (such as photosynthesis and sulphide oxidation) and

the fluxes of solutes and gases. As the skin circulation efficiently drives infiltration and mineralisation of dissolved organic carbon (DOC) and particulate organic carbon (POC), it promotes high primary productivity. The deep circulation and anaerobic degradation processes produce a sulphate-depleted and methane-enriched plume under the tidal flat surface (Beck et al. 2008), and (the development of) sulfidic and nutrient-rich seeps at the low water line (Billerbeck et al. 2006b; Al-Raei et al. 2009). How the organic material is transported from the sediment surface to a depth of several metres in the tidal flat needs further investigation.

This paper describes the dynamics of some key chemical parameters (mainly oxygen, sulphide and pH) in the surface sediments of a sloping intertidal flat with a maximum height of 1.5 m above the water level at low tide with the aim of giving insights into the importance of local and short timescale processes such as tides and hydrodynamic-pressure-driven transport. To obtain pore water data in a minimally invasive way, autonomous profilers mounted with microsensors were used. These time-resolved fine-scaled results are combined with nutrient analyses from pore waters that were extracted from selected sediment cores.

## 2 Materials and methods

### 2.1 Site description

The study site was located at the northeastern margin of the Janssand, an 11-km<sup>2</sup> intertidal sand flat in the back-barrier area of the island of Spiekeroog in the East Frisian Wadden Sea, Germany (53°44'07" N, 007°41'57" E). This site has also been the focus of other related studies, and a detailed description can thus be found in Billerbeck et al. (2006a, b) and Røy et al. (2008). The flat consists of an elevated upper flat which slopes towards the low water line (see Fig. 1). Three main zones were distinguished: (1) the upper flat, which was more or less horizontal; (2) the slope between the upper flat and the low water line; and (3) the low water line.

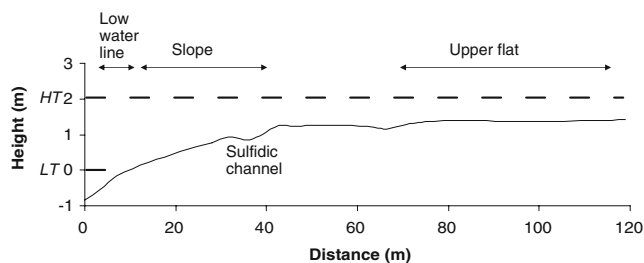


**Fig. 1** Topographic profile of the Janssand intertidal area indicating the zones indicated in the text. Two examples of water levels during low tide (LT) and high tide (HT) are indicated with dashed lines. The depression in the surface halfway the slope indicates a sulfidic channel

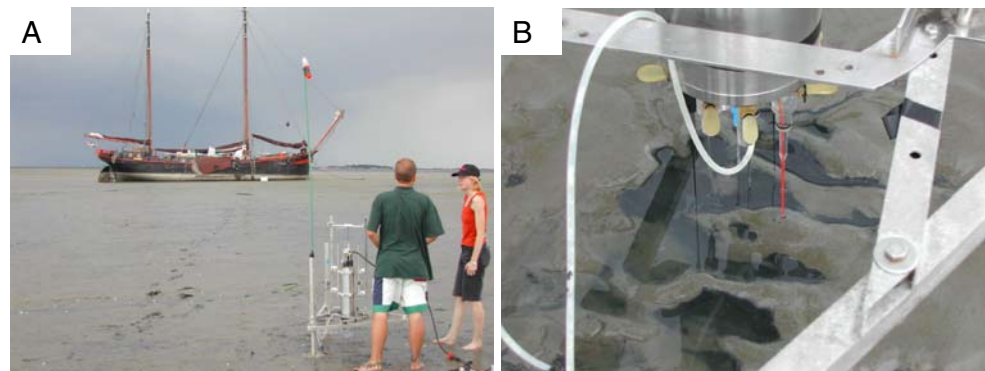
The distance between the upper flat and the low water line was approximately 50 m. The top was covered by 1.5 to 2 m of water during high tide and became exposed for 6 to 8 h during low tide depending on the tidal range. The site was visited in a number of approximately 2-week-long campaigns by using a flat bottom vessel that could fall dry during low tide (Fig. 2a).

The surficial sediment in the centre of the flat consisted of rather homogeneous yellow fine sand with signs of bioturbation/bioirrigation (e.g. polychaetes, *Arenicola*). The density of *Arenicola* in the upper flat in summer was estimated to be 3.6 individuals per square metre (Billerbeck et al. 2006b). On the slope between the upper flat and the low water line, numerous seeps and channels were observed, often associated with high levels of reduced compounds such as sulphide causing a dark colour of the surface sediment. Near the low water line, the sediment became more heterogeneous with discontinuous mud lenses intercalated below the surface. Seeps characterised by a strong sulfidic smell, gas bubbles and quick sands into which one could sink quite suddenly were encountered up to 30 m from the low water line (Fig. 3). Bioturbation was almost absent up to 50 m from the low water line, but became increasingly more abundant from approximately 100 m onward. In the seep-impacted areas, worms were almost absent in a 20- to 50-m-wide belt along the low water line: In summer, the density of *Arenicola* was counted to be approximately 0.6 individuals per square metre. At the same time, maximum densities of *Arenicola* increased to 3.6 individuals per square metre at a distance of approximately 60–100 m (Billerbeck et al. 2006b). In the central area of the flat, even higher densities were found. The sediment comprised well-sorted siliciclastic sand ( $\sigma < 0.38$  phi) with a mean grain size of 176  $\mu\text{m}$ . The permeability ranged between  $7.2 \times 10^{-12}$  m<sup>2</sup> at the upper flat and  $5.2 \times 10^{-13}$  m<sup>2</sup> at the low water line (Billerbeck et al. 2006a).

### 2.2 Sampling strategy

A general difficulty for measurements in permeable sediments is that the pore water composition is influenced by transport, and transport is influenced by the variable hydraulic regime. The hydrodynamics at the sediment–water interface are thus easily disturbed by the observation technique. Obviously, retrieval of sediments and chemical analysis of extracted pore water will not give any information about in situ dynamics. Benthic chambers seal off the sediment surface under investigation and replace the natural flow regime by an artificial one that depends on the rotation speed of the stirrer. In the present study, pore water data for selected dissolved species were measured in situ using autonomous profilers mounted with microsensors, a method which

**Fig. 2** **a** Vessel used for the field research with, in the foreground, the profiler deployed on the exposed flat. **b** Close-up of the profiler showing the micro-sensors above a sulfidic seep



is only minimally invasive and leaves the sediment surface exposed to winds, currents, waves and tides during the measurements. This setup allows for continuous profiling over whole tidal cycles and the evaluation of the corresponding pore water and element flux changes at the sediment–water interface. The time-resolved fine-scaled lander results are combined with nutrient analyses from pore waters that were extracted from selected sediment cores.

Measurements were performed at the upper flat, along the slope and at the low water line. The site was visited repeatedly between 2002 and 2006.

### 2.3 In situ microsensor measurements

In situ measurements of oxygen penetration depth were performed by microsensors mounted on an autonomous

profiler as described in Glud et al. (1999) and Wenzhöfer et al. (2000; Fig. 2b). Clark-type oxygen microelectrodes and amperometric  $H_2S$  microsensors were made and calibrated as described previously (Revsbech 1989; Jeroschewski 1996). Instead of using normal 5- to 10- $\mu m$  tips, the sensors were prepared with an approximately 300- $\mu m$  (200–500  $\mu m$ ) tip diameter to prevent breakage in the relatively firm sediment. Nevertheless, the actual sensing diameter was 2  $\mu m$  with less than 5-s response time ( $t_{90}$ ). Electrodes used for pH measurements were liquid ion-exchange membrane microelectrodes (De Beer 2000) with a 200- $\mu m$  tip size and an agar reference and a commercial glass electrode (3-mm tip diameter, InLab 423, Mettler Toledo, Switzerland). For temperature measurements, a Pt100 electrode (Umweltsensortechnik, Germany) was used. The position of the sediment surface was monitored with a resistivity microelectrode as described by Glud et al.

**Fig. 3** Examples of large and small sulfidic pools and streams



(2009). To correct for uneven surface topographies, the results of the resistivity measurements were compared to analogous indications inferred from the signals of the other sensors.

The profiler was placed on the flat during low tide with the microsensors initially positioned 1 to 2 cm above the sediment surface (Fig. 2b). Profiles were measured over at least one tidal cycle to a sediment depth of 6 cm at 1-mm intervals. Repeated profiles were measured every 20 to 60 min. The sensors sometimes produced persistent holes in the sediment during low tide; such profiles were discarded from the data set.

#### 2.4 Photopigment analysis

Photopigments in the sediment were collected and analysed as described by Billerbeck et al. (2007). The top 12 cm of the sediment was sectioned at 1-cm intervals down to 2-cm depth and at 2-cm intervals below. The sediment samples were kept frozen and in darkness until analysis. Pigments were extracted in the laboratory by sonification of sediment subsamples in 10 ml 90% acetone and subsequently measured in the supernatant on a Shimadzu UV-160A spectrophotometer. Concentrations of fucoxanthine, diadinoxanthine, chlorophyll A and phaeophytin A were determined by comparison to simultaneously measured standards.

#### 2.5 Nutrient profiles

Sediment was sampled at low tide using core liners of 3.6- and 5.4-cm inner diameter for porosity and pore water extraction, respectively. Cores for pore water extraction were immediately sliced inside a glove bag filled with argon gas. The slices, 1-cm steps up to 14-cm depth (March 2004) or 6-cm depth, and 2 cm up to 18-cm depth thereafter, were transferred into closed containers and centrifuged for 20 min at 4,000 rpm. After filtration through 0.2 µm (Millex GP and nylon) syringe filters, aliquots of pore water were kept frozen in plastic centrifuge tubes (Eppendorf) for spectrophotometrical nutrient determination (silicate, phosphate, ammonium, nitrate and nitrite) with a Skalar continuous-flow analyser according to Grasshoff et al. (1999). Samples for dissolved inorganic carbon (DIC) were preserved with saturated mercuric chloride solution and stored in glass vials until analysis. DIC analysis was performed by flow injection (Hall and Aller 1992). Dissolved sulphide was determined from samples fixed with 5% zinc acetate solution and stored frozen for subsequent spectrophotometrical analysis (Shimadzu UV-160A spectrophotometer) with the methylene blue method (Cline 1969).

### 3 Results and discussion

#### 3.1 Skin circulation

The oxygen dynamics in the upper few centimetres were clearly determined by the hydrodynamics (Fig. 4). During low tide, oxygen hardly penetrated into the sediments. During high tide, on the other hand, oxygen penetrated several centimetres in a very dynamic way. Obviously, the penetration could rapidly increase in response to stronger currents and wave action. The patterns observed by separate sensors installed on the same profiler were similar, indicating that the dynamics were indeed caused by hydraulics and not by increased bioturbation.

The oxygen dynamics were similar at all locations on the Janssand (Fig. 4a, b). No clear differences were observed in oxygen penetration depths at the low water line, along the slope or on the upper flat (Fig. 4b). At low tide, oxygen penetrated 5 to 10 mm, whereas at high tide, a penetration of several centimetres was usually observed. This indicates that currents can drive water from the water column into the sediments to a depth of at least 5 cm, and probably more, at all three sites. This is a perfect illustration of skin circulation driven by currents over ripples (Huettel et al. 1998; De Beer et al. 2005; Billerbeck et al. 2006a). The permeability near the low water line was a bit lower than at the top of the flat, but this did not result in substantially less advective oxygen penetration; apparently, the hydrodynamic pressure due to tides and water movement is more decisive for the oxygen penetration depth.

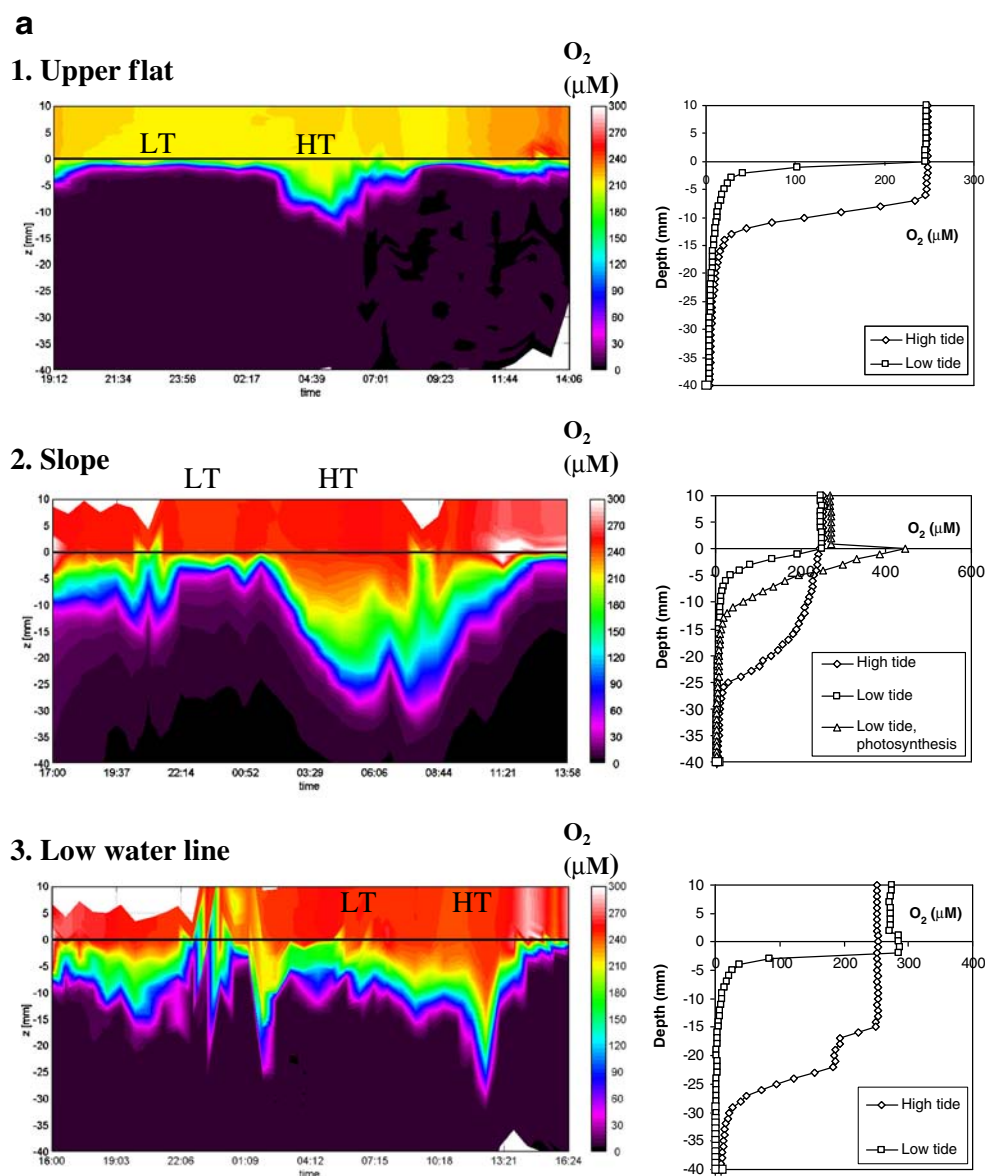
On several occasions, seasonal effects in oxygen penetration were observed. Generally, the penetration was deeper during winter and spring than during summer (exemplified by Fig. 5). This is explained by lower respiratory activity during spring and the much higher oxygen levels in the colder water column: Per volume pore water that was exchanged, more oxygen entered the sediments and was more slowly consumed, thus penetrating deeper. In addition, a higher frequency of strong winds, higher current speeds and resuspension events caused deeper oxygenation of the sediments at all sites in spring.

Both Figs. 4 and 5 show high oxygen concentrations in the top centimetre during low tide, a feature which will be addressed further down.

#### 3.2 Deep circulation

Whereas the oxygen dynamics were rather similar at the three sites, clear differences were observed when also sulphide and pH were measured (Fig. 6). No sulphide was measured in the central areas of the flat, but high sulphide levels were observed near the low water line. The pH in deeper anoxic zones of the central area was approximately

**Fig. 4 a** Oxygen dynamics at upper flat, slope and low water line illustrated by contour plots and some indicative profiles, March 2006. *HT* high tide, *LT* low tide. **b** Oxygen penetration depths at various sites (upper flat, low water line and slope). Data from two separate sensors (nos. 8 and 12) installed on the same autonomous profiler are shown. High tide and low tide are indicated with *HT* and *LT*, respectively

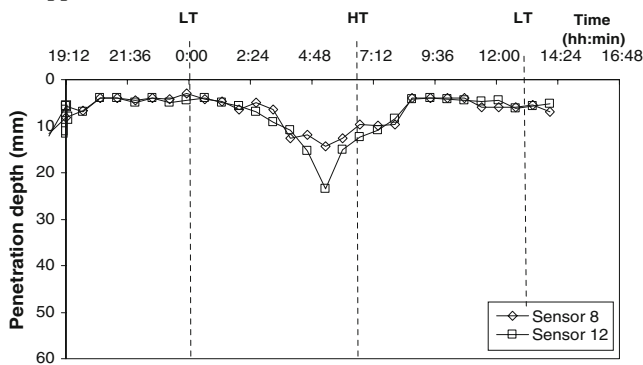


7.6 and showed a dip just below the surface where oxygen disappeared. This pH minimum was probably caused by aerobic respiration, most probably with organic matter as electron donor. The pH in the deeper sediments at the low water line was much lower than in the central area, reaching values of 7.3, no dip being observed at the oxic–anoxic interface. The reason for the low pH is not clear, but a rather low pH is also typical for deep-sea seeps (Aloisi et al. 2004; De Beer et al. 2006; Torres et al. 2004; Wallmann et al. 2006). Aerobic respiration could not drive the pH down and induce a pH minimum due to the very high DIC levels in the seeps that, at pH 7, act as an effective pH buffer. DIC reached concentrations up to or even exceeding 20 mM in the seep fluids and less than 5 mM DIC in the pore water of central areas (Billerbeck et al. 2006b; Al-Raei et al. 2009). Carbon isotope measurements indicate that the oxidation of

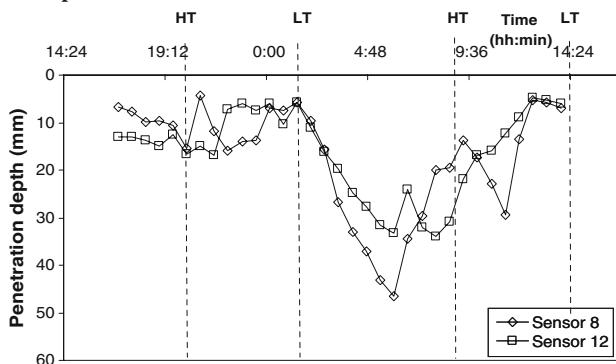
methane contributes significantly to the enhanced DIC contents at the seeps (Böttcher et al. 2007). Surficial and deep pore water circulation governs spatial and temporal scales of nutrient recycling in intertidal sand flat sediment. Interestingly, the pH and sulphide concentrations in the pore water near the low water line were highly dynamic and strongly influenced by the tides. This is very clearly illustrated by the separate profiles in Fig. 6a, b and the contour plots in Fig. 6b. During low tide, sulphide reached the sediment surface, whereas at high tide, sulphide did not reach the surface and was probably oxidised within the sediment by oxygen or precipitated by iron. This is concurrent with the model that at low tide, the pressure head drives pore water through the deeper sediments of the flats towards the low water line, whereas at high tide, the pressure head is dissipated and the seepage stops.

**b**

**1. Upper flat**



**2. Slope**



**3. Low water line**

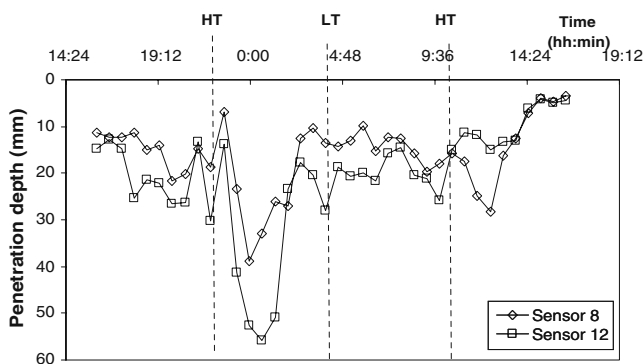
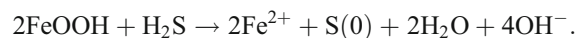
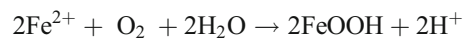


**Fig. 4** (continued)

Pore water, in particular, seeps out of the flats from depressions such as pools and shallow channels. The channels are cut into the flat by water draining from the central areas of the flats during low tide. Pools of various sizes were found, ranging from 20-cm diameter and 10-cm depth to 4-m diameter and 1-m depth. How these pools were formed is not obvious. As shown by Røy et al. (2008), deep pore water flow is driven by the pressure head between the water residing at the top of the flat during low tide and the seawater (Fig. 7 shows the film of water left on the upper flat during low tide). As the pore water flow is pressure-driven, the path of the lowest resistance will be

preferred and the shortest path will thus have the highest flow velocity. Depressions such as pools, priels or channels will therefore ‘attract’ the pore water seeping towards the low water line (Fig. 3).

The seeps, which are easily identified by the development of black FeS precipitates, occur along the low water line and at the middle of the slope. Profiles of H<sub>2</sub>S, O<sub>2</sub> and pH (Fig. 8a, b) demonstrate some typical features. H<sub>2</sub>S can reach very high values up to just below the sediment surface (mM range). In pools that are stagnant during low tide, sulphide can also be found in the water column. In July 2003 (data not shown), concentrations of approximately 30–360 μmol total sulphide were found in the overlying water of a stagnant pool. Here, the availability of reducible iron in the sediment was completely exhausted (Bosselmann et al., in preparation) and the oxidation rate of sulphide was lower than the supply rate. Sulphide, therefore, was able to leave the sediment and accumulate in the overlying water. The co-occurrence with milky elemental sulphur indicates that sulphide oxidation to intermediate sulphur species took place (Böttcher et al. 1998). The sulphide and oxygen profiles in the surface sediment were sometimes separated by a few centimetres (Fig. 8a). This indicates that in these cases, the sediment contained sufficient iron oxides to react with the upwelling sulphide. This is in stark contrast to the data mentioned above where the pool of reducible iron in the sediment was exhausted. Apparently, the amount of reducible iron in the sediment changes from place to place. This is not unexpected because of the frequent reworking of the sediment during which re-oxidation can take place and the spatially variable supply of sulphide. Oxygen, the terminal electron acceptor for sulphide leaking out of the sediments, became slowly depleted from the overlying water in pools during low tide. The sulphide gradients were often very steep near the surface, but leveled off below the upper centimetre (Fig. 8). In other cases, sulphide profiles showed a transient maximum in the course of the measurement cycle. These phenomena clearly indicate that the sediments below the stagnant pools are far from a steady state. In most cases, no dissolved sulphide could be found in the overlying water (example: October 2004, Fig. 8), but sulphide was converted into sulphur, resulting in a milky overlying water body. Most probably, the oxidation of sulphide to sulphur in the pools is chemically catalysed by Fe via a series of reactions (Dos Santos and Stumm 1992):



However, microbial oxidation cannot be excluded. Indeed, algae that were growing in sulfidic streams were

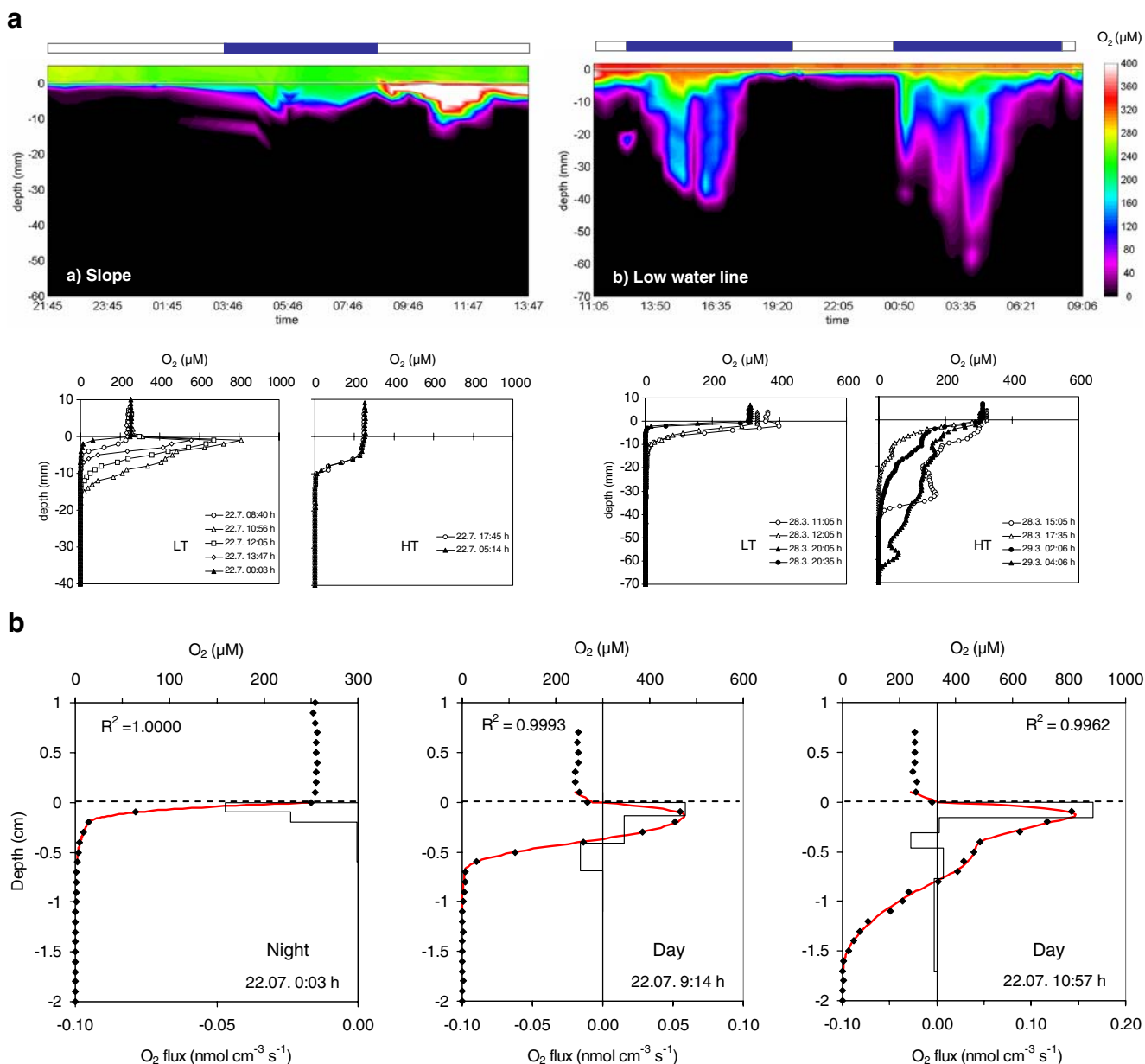


**Fig. 5** Impact of weather and tides. **a** Summer situation on the sand flat (July 2003, slope) with high photosynthetic activity during low tide. **b** Very high oxygen penetration depth following a storm event (March 2004, low water line). Exemplary single profiles are shown for low tide (LT) and high tide (HT) during day and nighttime (light and dark symbols, respectively). Low tide oxygen fluxes (consumption, production rates) from July 2003 (slope) calculated using Profile (Berg

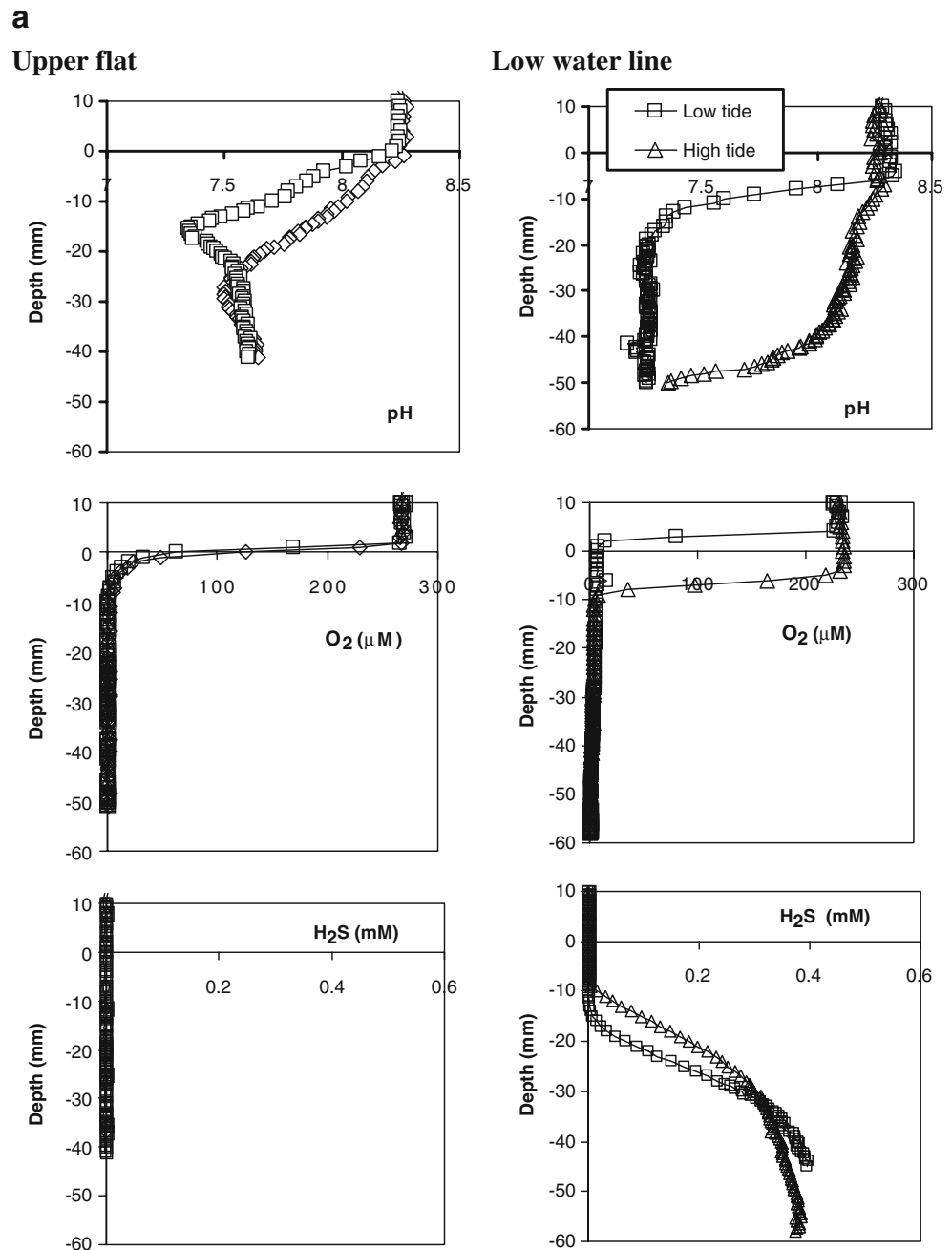
et al. 1998). The dashed line indicates the sediment surface, symbols measured concentrations, the red line the model simulation. Production/consumption zones are presented as black rectangles. The profile measured at 1057 hours shows an impact of drainage transport with oxygen production below the light penetration depth of approximately 3 mm

covered by filamentous sulphur bacteria (Fig. 9). In the absence of such holdfasts, these *Thiotrix*-like organisms would not be able to sustain. Upon transfer of sulfidic sediments to a laboratory flume, extensive *Arcobacter* mats developed within hours and then disappeared within approximately 1 day (data not shown). These sulphide oxidisers seem related to the ‘Harold’ organisms that produce filamentous sulphur (Wirsen et al. 2002).

The sulfidic channels mainly occur along the slope of the flat. The dynamics of sulphide and oxygen (Fig. 10) are similar to those in the sulfidic pools; however, adjacent  $O_2$  and  $H_2S$  profiles are similar and often overlap. Due to this overlap, biological oxidation of sulphide is more likely here than in the stagnant pools, and indeed, the filamentous bacteria were most often found in these streams.  $H_2S$ ,  $O_2$  and pH profiles moved in response to the tides, especially the  $H_2S$  profiles.



**Fig. 6 a** Difference between pH, oxygen and sulphide dynamics between upper flat and low water line exemplified by profiles, July 2005. The data for the upper flat are two subsequent profiles around high tide, the data for the low water line are around low tide and around high tide. **b** Dynamics at low water site demonstrated by data from 27 October 2005. *HT* high tide, *LT* low tide



Apart from elevated concentrations of sulphide, elevated concentrations of nutrients and DIC were also found in seeps (Fig. 11). Sulfate was depleted, again showing that the seeps are exit points for degradation products, with high pore water concentrations of these degradation products in the lower sand flat (>6 mM sulphide, 19 mM DIC, up to 4 mM NH<sub>4</sub> and 0.7 and 1 mM PO<sub>4</sub> and silicate, March 2004). Fe<sup>2+</sup> and Mn<sup>2+</sup> concentrations were lower than in the centre sediments (Bosselmann et al., in preparation), probably due to precipitation as sulphides and carbonates or because of

an already depleted sedimentary Mn pool. The seeps were surprisingly high in organic matter, 0.25% to 0.85% in the upper 3 cm of a seep, i.e. much higher than in the central flat where 0.06–0.13% was observed (Billerbeck et al. 2006b; Al-Raei et al. 2009). This may indicate preferential burial of organic matter at the low water line, which might be due to lower hydrodynamics at low tide and temporal burial of macroalgae.

The seeps are not a constant phenomenon but display dynamics that are much slower than the seasonal time cycle and are certainly not in phase with the seasons. Billerbeck

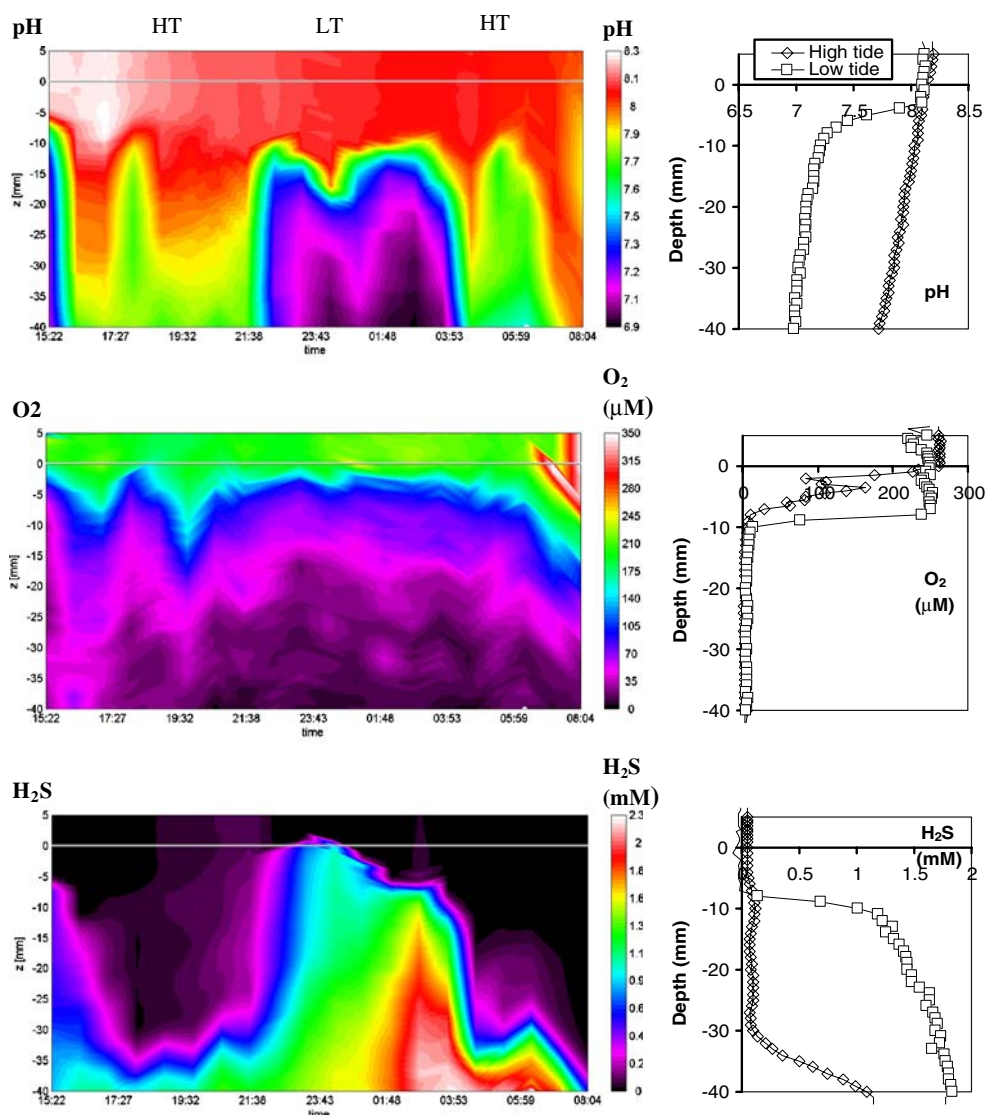


Fig. 6 (continued)

et al. (2006a) found that at one location, nutrient concentration fluctuated with a rhythm of approximately 1.5 years. This is consistent with the notion that seep chemistry is not determined by local processes but by a distant and deep source. The fluctuations in pore water chemistry can be attributed to slow changes in transport which, in turn, are influenced by the surface topography that changes slowly due to erosion and sedimentation or sometimes more dramatically during periods of enhanced hydrodynamics (e.g. storm events).

Of course, some short-term effects can be observed from extreme weather conditions. For example, no accumulation of degradation products was observed in oxic surface sediments at the low water line directly after a storm (Fig. 5). However, this is a very transient phenomenon.

The onset of pore water seepage as soon as the upper flat falls dry is also illustrated in Fig. 5b with the fast reduction

of the oxygen penetration depth at the low water line shortly after falling tide.

### 3.3 Photosynthesis

During illumination, distinct oxygen peaks were often observed at the sediment surface, but illumination did not result in much deeper oxygen penetration. The data in Fig. 5a show very nicely the effect of light on the oxygen profiles. During very calm conditions in summer, depth-integrated  $O_2$  production, as inferred from the gradients using PROFILE (Berg et al. 1998), was very high. Production increased from  $6.8 \text{ mmol m}^{-2} \text{ day}^{-1}$  (early morning) to  $17 \text{ mmol m}^{-2} \text{ day}^{-1}$  (midday). Most profiles cannot be explained by diffusion alone, thus reflecting non-steady state due to rapidly changing light conditions and transport rates during low tide which complicate the



**Fig. 7** The central area of the Jansand during the later period of low tide. Note that the flat is covered with a thin water layer throughout the whole low tide period

determination of the actual in situ photosynthetic  $O_2$  production. We expected a higher photosynthetic activity near the seeps, as these are a source of nutrients. Superficial inspection also indicated more diatoms and, in summer only, green flagellates. However, photosynthetic activity did not seem higher near seeps (production was of the same order of magnitude with up to  $10.3 \text{ mmol m}^{-2} \text{ day}^{-1}$  but restricted to single events in a consumption-dominated environment). More detailed observations indicate that the sulphide is inhibitive for phototrophs. A gradient of various dissolved compounds and photopigments across a sulfidic channel shows the vulnerability of the microalgal population to the sulphide: At the middle of the channel, where sulphide is highest, all photopigments show a minimum (Fig. 12). It therefore seems that the observation that more diatoms are present near the low water line is misleading: Possibly, they are more exposed and clustered in patches, as they escape the sulfidic sediments, and are thus more visible than on non-sulfidic sediments higher up the flat. Interesting is that during warm summer days, a second phototrophic population developed. Bright green coatings of green flagellates only developed near seeps; however, these organisms also avoided direct exposure to sulphide. Interestingly, the green algae and the yellow brown diatoms remained separated, on account of which, a colorful mosaic develops which follows the micro-topography of ripples and gullies.

#### 4 Summary and conclusions

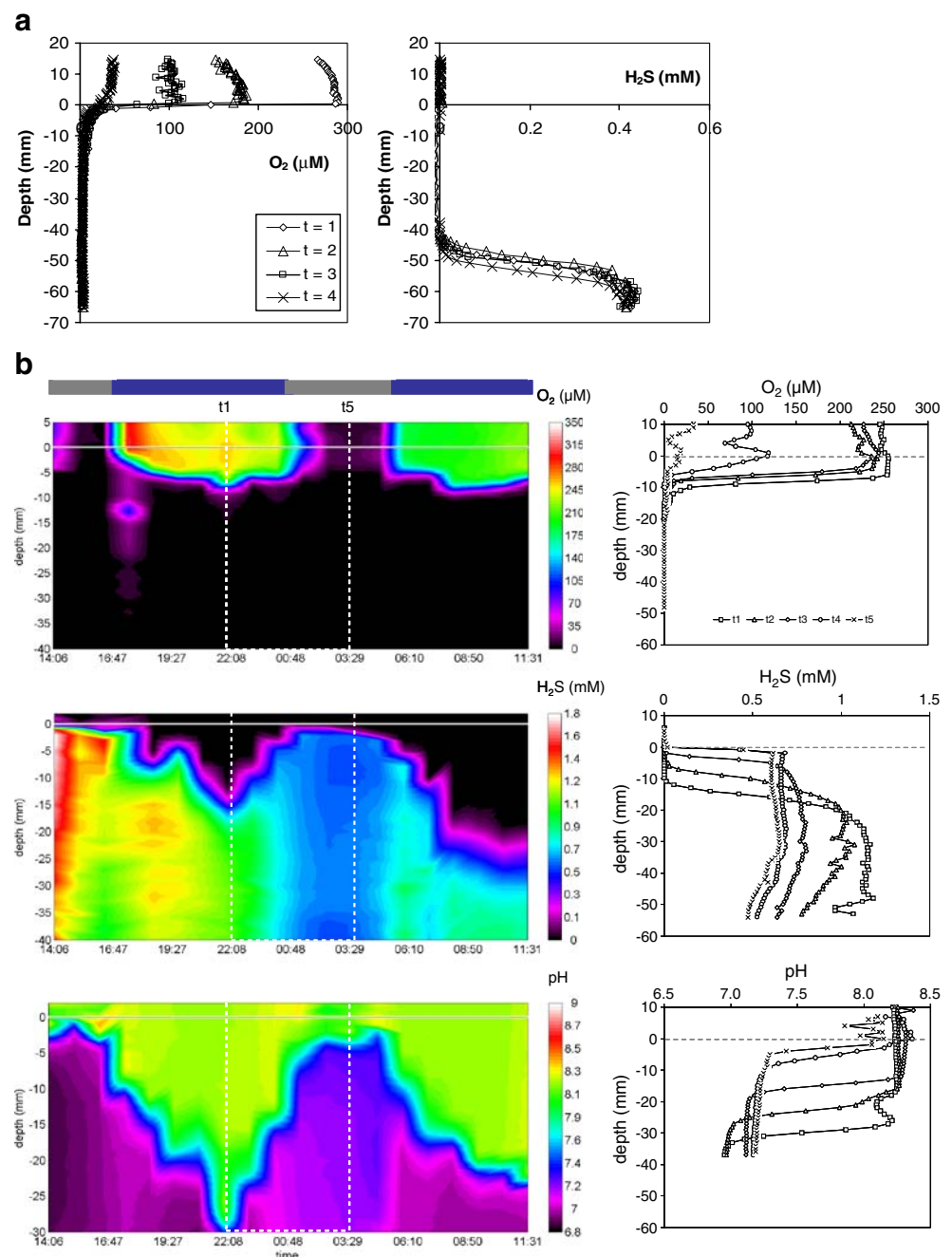
The results presented in this paper clearly demonstrate the high dynamics of oxygen, sulphide and pH in the surface sediments of an intertidal flat.

Due to advective transport, intensive skin circulation occurs which gives rise to strong interaction of solutes in the surface sediments. This leads to rapid exchange between organic matter and oxygen in the surface sediments. The results obtained are in line with other recent findings showing that sandy sediments can be more productive than previously thought because of their functioning as filters (e.g. De Beer et al. 2005; Werner et al. 2006). Values for the oxygen consumption at the surface under the control of these processes were estimated for the site by Billerbeck et al. (2006b). This demonstrated that rates during inundation were significantly higher than under exposure, emphasising the importance of advective transport as compared to diffusive transport.

Next to this filtering in the surface sediments, which occurs more or less over the whole surface, localised seeps were observed with high concentrations of reduced compounds (such as sulphide) and nutrients. It was demonstrated that these too are subject to dynamics, controlled mainly by tides. Together with earlier publications (e.g. Billerbeck et al. 2006b; Røy et al. 2008), these results show the importance of these seeps as sources of reduced compounds.

The data clearly confirm how the two main transport processes shape the chemical and microbial architecture of a permeable sand flat. Skin circulation is an efficient filter for DOC and POC from the water column and transport of oxygen into the sediments. This is the reason for the high areal mineralisation rates of permeable sands. Most of the labile particulate organic matter is degraded aerobically in the surface sediment in the order of days. This is supported by a wave-tank study of Franke et al. (2006) who detected high oxygen consumption downstream of hotspots of buried labile organic matter. Local bacterial decomposition of POM is spatially decoupled from the final degradation of dissolved organic matter by pore water flow. DOM is efficiently distributed over larger sediment volumes, thereby enhancing overall mineralisation processes leading to a mosaic of suboxic and anoxic microniches despite the exposure to oxygenated pore water. Furthermore, fluctuating redox conditions, as observed with the tidally dependent oxygen penetration depth in combination with sediment reworking due to bioturbation and resuspension, have been shown to enhance the overall mineralisation rates as well as extend oxygen exposure times to OM which, under diffusion-controlled conditions, would have been buried in an anoxic environment (Meile and Van Cappellen 2005). Deeper bioirrigation and sediment reworking by *Arenicola marina* is probably of minor importance at this study site with rather high-energy hydrodynamics. *A. marina* is relatively rare with approximately four individuals per square metre (determined in summer 2003, Billerbeck et

**Fig. 8** **a** Oxygen and sulphide dynamics in a sulfidic pool (data: November 2004). At  $t=1$ , the pool was still in contact with the sea (high tide); from then on ( $t=2$  to 4), the pool became disconnected and the oxygen concentration in the pool started to decrease. **b** Tidal dynamics of  $O_2$ ,  $H_2S$  and pH in a small sulfidic pool (Oct. 2002). Profiles on the *right* are extracted from the contour plot and visualise the change from high tide (*dark bar*) to low tide (*light bar*) from 2200 to 0330 hours.  $H_2S$  concentrations above 1 mM are beyond the linear calibration range and represent only minimum concentrations. Note the different depth scales

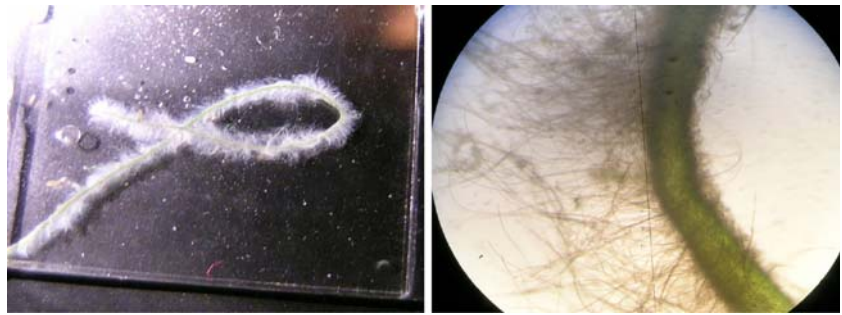


al. 2006b) as compared to other areas with 40–80 individuals of bioturbators per square metre (Kristensen 2001). The importance of bioirrigation for oxygen dynamics can be estimated as follows: For each worm, we can assume a pumping rate of approximately  $90 \text{ ml h}^{-1}$  for approximately  $10 \text{ h day}^{-1}$  during inundation (Billerbeck et al. 2006b). Using these values, and an oxygen concentration in the water of  $240 \text{ } \mu\text{M}$ , the rate of oxygen input due to bioirrigation is estimated to be  $240 \text{ } \mu\text{M} \times 3.6 \text{ individuals per square metre} \times 90 \text{ ml h}^{-1} \text{ per individual} \times 10 \text{ h day}^{-1} = 0.8 \text{ mmol m}^{-2} \text{ day}^{-1}$ , which is small compared to the areal oxygen consumption rates reported for

the site by Billerbeck et al. (2006b; in the order of  $30\text{--}260 \text{ mmol m}^{-2} \text{ day}^{-1}$ ). Even in the case of ten times higher bioirrigation densities, the importance of bioirrigation for overall oxygen dynamics would still be small compared to the overall advective transport. In sites with low-energy hydrodynamics, less permeable sediment and more bioirrigating organisms, bioirrigation will be driving a larger fraction of the total oxygen exchange.

A further fraction of the filtered organic matter somehow arrives up to several metres depth within the sand flat where it is degraded by a suite of anaerobic processes, mainly sulphate reduction and methanogenesis. Due to the deep

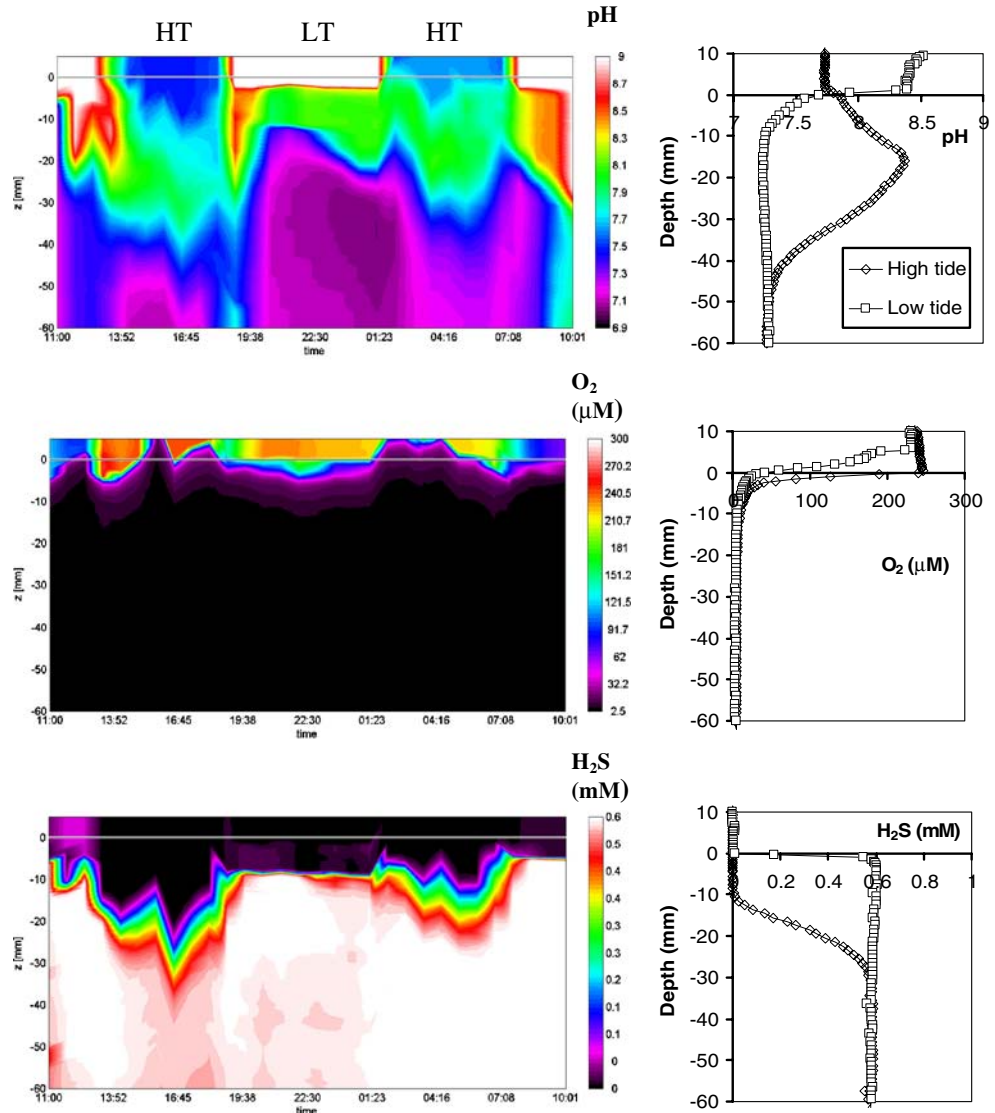
**Fig. 9** Algae grown in a sulfidic stream were covered by filamentous sulphur bacteria



body circulation, the degradation products (nutrients, DIC, methane and sulphide) leave the flat at the points where the deep circulation ends, namely in seeps at the low water line. These two transport processes shape the distribution of mineralisation processes. Whereas in the top 3–5 cm of the flat aerobic mineralisation is the main pathway, sulphate

reduction leads to depletion of sulphate deep within the flat, as a consequence of which, methanogenesis becomes possible. The products of these processes are partially oxidised by microbial and chemical processes at the seeps. The seeps are probably important sources for methane, a powerful greenhouse gas. Apparently, the methane oxidising

**Fig. 10** Sulfide, oxygen and pH dynamics in a sulfidic channel (March, 2005). *HT* high tide, *LT* low tide



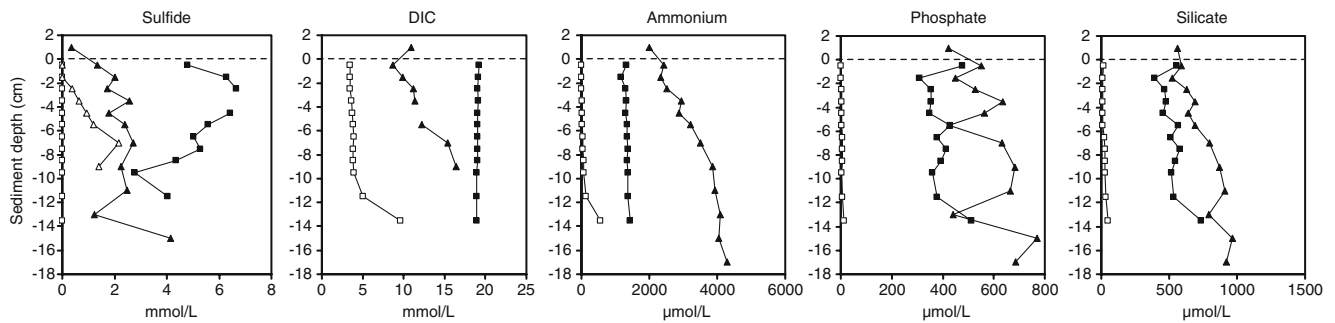


**Fig. 11** Selected pore water concentrations of reduced (*dark symbols*) and surrounding oxic (*light symbols*) surface sediments in July 2003 (*triangles*) and March 2004 (*rectangles*). No DIC and nutrient data are

available for the oxic reference in July. The *dashed line* denotes the sediment surface

capacity does not develop fast enough in this dynamic environment to effectively consume the emitted methane.

This study clearly shows strong differences in local environmental conditions. These are expected to have a huge impact on the biology. One example of this was shown in Fig. 12: Photopigments show a decreased level of algae at a site with high sulphide. Another example is the impact on of seepage on bioirrigation. At the same time, organisms are expected to adapt or even profit from

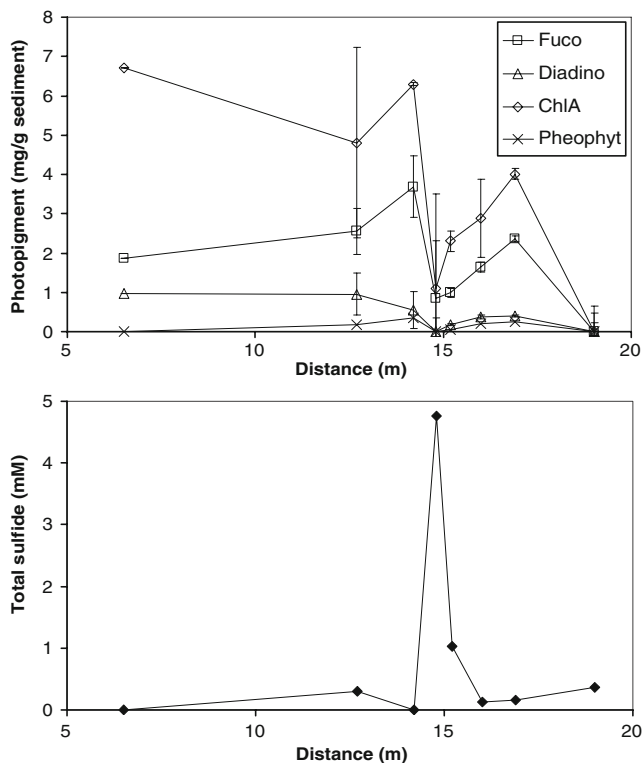


**Fig. 12** Concentrations of photopigments and total dissolved sulphide measured along a transect perpendicular to a sulfidic creek. *Fuco* fucoxanthine, *Diadino* diadinoxanthine, *ChlA* chlorophyll A, *Phaeophyt* phaeophytine A. Note the low photopigment levels at the sulphide maximum. Sulphide was measured in pore water at 3-cm depth

these local conditions. For instance, motile sulphide-oxidising organisms are expected to be present at sites with high sulphide outflow. Also, anaerobic methane oxidation is expected to play a role at these sites with elevated levels of sulphate and methane brought together. Ishii et al. (2004) found aggregates of sulphate-reducing bacteria and archaea in sediment from the study site (September 2002) strongly resembling consortia involved in anaerobic methane oxidation found in sediments near methane hydrate deposits. These occurred in depths >12 cm, but not in black spots, i.e. sulphate-depleted areas where the methane is produced. Total cell counts showed maxima in the upper 2- to 3-cm depth, including *Desulfohalobaceae* which were found only here. Planctomycetes, presumably aerobic heterotrophic bacteria which are characteristic for permeable sediments with higher  $O_2$  penetration depth (Musat et al. 2006), were present in high abundance at all depths but with a maximum in 3–4 cm. This reflects the maximum penetration depth at the site. Black spots were also characterised by high bacterial numbers, except for *Desulfosarcinales* which showed their lowest abundance there (Ishii et al. 2004).

The data presented in this paper focused on the top layers of the sediments. Next to this, high activity was demonstrated for the same site in deeper sediment layers (upper 5 m), especially in the sulphate–methane transition zone (e.g. Wilms et al. 2006, 2007; Røy et al. 2008). These results demonstrate that microbial communities occur in a stratified manner at the study site and that these are combined with flow patterns which may lead to the transport of reduced compounds to the top layer. Once the compounds have reached the upper layers, the biogeochemical processes discussed in this paper further transform the compounds before their final release into the seawater or atmosphere. As the fluxes are a result of processes at the surface and at greater depth, a complete quantitative evaluation must encompass all of these processes.

**Acknowledgements** We thank Ronald Monas and Iso Speck and the crews of the Twee Gebroeders and Verandering for letting us make use of their ships and their help and Ingrid Dohrmann for microsensor construction and help in the field. We thank Rodrigo da Purificação for photopigment analysis and help in the field. We also gratefully acknowledge the support of others involved in microsensor construction (Gaby Eickert, Ines Schroeder, Anja Eggers, Karin Hohmann), help with sample analysis (Martina Alisch, Daniela Franzke, S. Lilienthal, A. Schipper) and technical assistance of Volker Meyer, Paul Faerber, Harald Osmers, Jens Langreder, Georg Hertz and Alfred Kutsche. We thank Filip Meysman and one anonymous reviewer for their comments. The study was supported by German Science Foundation during DFG research group “Biogeochemistry of Tidal Flats” (JO 307/4, BO 1584/4) and the Max Planck Society. We wish to thank J. Rullkötter for the coordination of the research group and B.B. Jørgensen for his continuous support of the project.

**Open Access** This article is distributed under the terms of the Creative Commons Attribution Noncommercial License which permits any noncommercial use, distribution, and reproduction in any medium, provided the original author(s) and source are credited.

## References

- Aller RC (2001) Transport and reactions in the bioirrigated zone. In: Boudreau BP, Jørgensen BB (eds) The benthic boundary layer. Oxford University Press, Oxford
- Alloisi G, Drews M, Wallmann K, Bohrmann G (2004) Fluid expulsion from the Dvurechenskii mud volcano (Black Sea). Part I. Fluid sources and the relevance to Li, B, Sr, I and dissolved inorganic nitrogen cycles. *Earth Plan Sci Lett* 225:347–363
- Al-Raei AM, Bosselmann K, Böttcher ME, Hespeneheide B Tauber F (2009) Seasonal dynamics of microbial sulfate reduction in temperate intertidal surface sediments: controls by temperature, sedimentology, and organic matter load. *Ocean Dynamics* (in press)
- Asmus R, Jensen MH, Mruphy D, Doerffer R (1998) Primary production of microphytobenthos, phytoplankton and the annual yield of macrophytic biomass in the Sylt-Rømø Wadden Sea. In: Gätje C, Reise K (eds) The Wadden sea ecosystem—exchange, transport and transformation processes. Springer, Berlin, pp 367–391
- Beck M, Dellwig O, Liebezeit G, Schnetger B, Brumsack HJ (2008) Spatial and seasonal variations of sulfate, dissolved organic carbon, and nutrients in deep pore waters of intertidal flat sediments. *Est Coast Shelf Sci* 79:307–316
- Berg P, Risgaard-Petersen N, Rysgaard S (1998) Interpretation of measured profiles in sediment pore water. *Limnol Oceanogr* 43(7):1500–1510
- Billerbeck M, Røy H, Bosselmann K, Huettel M (2007) Benthic photosynthesis in submerged Wadden Sea intertidal flats. *Est Coast Shelf Sci* 71:704–716
- Billerbeck M, Werner U, Bosselmann K, Walpersdorf E Huettel M (2006a) Nutrient release from an exposed intertidal sand flat. *Mar Ecol Prog Ser* 316:35–51
- Billerbeck M, Werner U, Polerecky L, Walpersdorf E, De Beer D Huettel M (2006b) Surficial and deep pore water circulation governs spatial and temporal scales of nutrient recycling in intertidal sand flat sediment. *Mar Ecol Prog Ser* 326:61–76
- Böttcher ME, Al-Raei AM, Hilker Y, Heuer V, Hinrichs KU, Segl M (2007) Methane and organic matter as sources for excess carbon dioxide in intertidal surface sands: Biogeochemical and stable isotope evidence. *Geochim Cosmochim Acta* 71:A111
- Böttcher ME, Oelschläger B, Höpner T, Brumsack HJ, Rullkötter J (1998) Sulfate reduction related to the early diagenetic degradation of organic matter and “black spot” formation in tidal sandflats of the German Wadden sea: stable isotope ( $^{13}\text{C}$ ,  $^{34}\text{S}$ ,  $^{18}\text{O}$ ) and other geochemical results. *Org Geochem* 29:1517–1530
- Böttcher ME, Hespeneheide B, Llobet-Brossa E, Beardsley C, Larsen O, Schramm A, Wieland A, Böttcher G, Berninger UG, Amann R (2000) The biogeochemistry, stable isotope geochemistry, and microbial community structure of a temperate intertidal mudflat: an integrated study. *Cont Shelf Res* 20:1749–1769
- Cline JD (1969) Spectrophotometric determination of hydrogen sulfide in natural waters. *Limnol Oceanogr* 14(3):454–458
- D’Andrea AF, Aller RC, Lopez GR (2002) Organic matter flux and reactivity on a South Carolina sandflat: the impacts of pore water advection and macrobiological structures. *Limnol Oceanogr* 47:1056–1070
- De Beer D (2000) Potentiometric microsensors for in situ measurements in aquatic environments. In: Buffle J, Horvai G (eds) In situ monitoring of aquatic systems: chemical analysis and speciation. Wiley, Chichester, pp 161–194
- De Beer D, Sauter E, Niemann H, Kaul N, Foucher JP, Witte U, Schlüter M, Boetius A (2006) In situ fluxes and zonation of microbial activity in surface sediments of the Håkon Mosby Mud Volcano. *Limnol Oceanogr* 51:1315–1331
- De Beer D, Wenzhöfer F, Ferdelman TG, Boehme SE, Huettel M, Van Beusekom J, Böttcher ME, Musat N, Dubilier N (2005) Transport and mineralization rates in north sea sandy intertidal sediments, Sylt-Rømø basin, Wadden sea. *Limnol Oceanogr* 50:113–127
- Dos Santos AM, Stumm W (1992) Reductive dissolution of iron(III) (hydr)oxides by hydrogen sulfide. *Langmuir* 8:1671–1675
- Franke U, Polerecky L, Precht E, Huettel M (2006) Wave tank study of particulate organic matter degradation in permeable sediments. *Limnol Oceanogr* 51:1084–1095
- Glud RN, Gundersen JK, Holby O (1999) Benthic in situ respiration in the upwelling area off central Chile. *Mar Ecol Prog Ser* 186:9–18
- Glud RN, Stahl H, Berg P, Wenzhofer F, Oguri K, Kitazato H (2009) In situ microscale variation in distribution and consumption of  $\text{O}_2$ : a case study from a deep ocean margin sediment (Sagami Bay, Japan). *Limnol Oceanogr* 54:1–12
- Grasshoff K, Kremling K, Ehrhardt M (1999) Methods of seawater analysis, 2nd edn. Wiley VCH, Weinheim
- Hall POJ, Aller RC (1992) Rapid, small-volume, flow injection analysis for  $\Sigma\text{CO}_2$  and  $\text{NH}_4^+$  in marine and freshwaters. *Limnol Oceanogr* 37:1113–1119
- Huettel M, Ziebis W, Forster S, Luther GW (1998) Advective transport affecting metal and nutrient distributions and interfacial fluxes in permeable sediments. *Geochim Cosmochim Acta* 62:613–631
- Ishii K, Mußmann M, MacGregor BJ, Amann R (2004) An improved fluorescence in situ hybridization protocol for the identification of bacteria and archaea in marine sediments. *FEMS Microbiol Ecol* 50:203–212
- Jeroschewski P (1996) An amperometric microsensor for the determination of  $\text{H}_2\text{S}$  in aquatic environments. *Anal Chem* 68(24):4351–4357
- Kristensen E (2001) Impact of polychaetes (*Nereis* spp. and *Arenicola marina*) on carbon biogeochemistry in coastal marine sediments. *Geochim Trans* 2:92–103
- Meile C, Van Cappellen P (2005) Particle age distributions and  $\text{O}_2$  exposure times: timescales in bioturbated sediments. *Glob Biogeochem Cycles* 19:GB3013. doi:10.1029/2004GB002371
- Meysman FJR, Galaktionov OS, Middelburg JJ (2005) Irrigation patterns in permeable sediments induced by burrow ventilation: a case study of *Arenicola marina*. *Mar Ecol Prog Ser* 303:195–212
- Meysman FJR, Galaktionov OS, Gribsholt B, Middelburg JJ (2006) Bioirrigation in permeable sediments: advective pore-water transport induced by burrow ventilation. *Limnol Oceanogr* 51:142–156

- Middelburg JJ, Nieuwenhuizen J, Iversen N, Hoegh N, De Wilde J, Helder W, Seifert R, Christoff O (2002) Methane distribution in European tidal estuaries. *Biogeochemistry* 59:95–119
- Musat N, Werner U, Knittel K, Kolb S, Dodenhof T, Van Beusekom JEE, De Beer D, Amann R (2006) Microbial community structure of sandy intertidal sediments in the North Sea, Sylt-Rømø Basin, Wadden Sea. *Syst Appl Microbiol* 29:333–348
- Precht E, Franke U, Polerecky L, Huettel M (2004) Oxygen dynamics in permeable sediments with wave-driven pore water exchange. *Limnol Oceanogr* 49:693–705
- Rasheed M, Badran MI, Huettel M (2003) Influence of sediment permeability and mineral composition on organic matter degradation in three sediments from the Gulf of Aqaba, Red Sea. *Estuar Coast Shelf Sci* 57:369–384
- Revsbech NP (1989) An oxygen microsensor with a guard cathode. *Limnol Oceanogr* 34:474–478
- Røy H, Lee JS, Jansen S, De Beer D (2008) Tide-driven deep pore-water flow in intertidal sand flats. *Limnol Oceanogr* 53:1521–1530
- Thibodeaux LJ, Boyle JD (1987) Bedform-generated convective-transport in bottom sediment. *Nature* 325:341–343
- Torres M, Wallmann K, Trehu AM, Bohrmann G, Borowski WS, Tomaru H (2004) Gas hydrate growth, methane transport, and chloride enrichment at the southern summit of hydrate ridge, Cascadia margin off Oregon. *Earth Planet Sci Lett* 226:225–241
- Van Beusekom JEE, Brockmann UH, Hesse KJ, Hickel W, Poremba K, Tillmann U (1999) The importance of sediments in the transformation and turnover of nutrients and organic matter in the Wadden Sea and German Bight. *Dtsch Hydrogr Z* 51:245–266
- Wallmann K, Drews M, Aloisi G, Bohrmann G (2006) Methane discharge into the Black Sea and the global ocean via fluid flow through submarine mud volcanoes. *Earth Planet Sci Lett* 248:544–559
- Wenzhöfer F, Holby O, Glud RN, Nielsen HK (2000) In situ microsensor studies of a shallow hydrothermal vent at Milos, Greece. *Mar Chem* 69:43–54
- Werner U, Billerbeck M, Polerecky L, Franke U, Huettel M, Van Beusekom JEE, De Beer D (2006) Spatial and temporal pattern of mineralization rates and oxygen distribution in a permeable intertidal sandflat (Sylt, Germany). *Limnol Oceanogr* 51:2549–2563
- Wetthey DS, Woodin SA, Volkenborn N, Reise K (2008) Pore water advection by hydraulic activities of lugworms, *Arenicola marina*: a field, laboratory and modeling study. *J Mar Res* 66:255–273
- Wilms R, Sass H, Köpke B, Cypionka H, Engelen B (2007) Methane and sulfate profiles within the subsurface of a tidal flat are reflected by the distribution of sulfate-reducing bacteria and methanogenic archaea. *FEMS Microbiol Ecol* 59:611–621
- Wilms R, Sass H, Köpke B, Köster J, Cypionka H, Engelen B (2006) Specific bacterial, archaeal, and eukaryotic communities in tidal-flat sediments along a vertical profile of several meters. *Appl Environ Microbiol* 72:2756–2764
- Wirsen CO, Sievert SM, Cavanaugh CM, Molyneux SJ, Ahmad A, Taylor LT, DeLong EF, Taylor CD (2002) Characterization of an autotrophic sulfide-oxidizing marine *Arcobacter* sp that produces filamentous sulfur. *Appl Environ Microbiol* 68:316–325